AMERICAN SOCIETY FOR MICROBIOLOGY | Antimicrobial Agents and Chemotherapy®

Acinetobacter baumannii Biofilm Formation in Human Serum and Disruption by Gallium

Federica Runci, Carlo Bonchi, Emanuela Frangipani, Daniela Visaggio, Paolo Visca

Department of Sciences, University Roma Tre, Rome, Italy

ABSTRACT Biofilm-associated infections caused by *Acinetobacter baumannii* are extremely recalcitrant to antibiotic treatment. We report that *A. baumannii* develops a mature biofilm when grown in complement-free human serum (HS). We demonstrate that 16 μM gallium nitrate (GaN) drastically reduces *A. baumannii* growth and biofilm formation in HS, whereas 64 μM GaN causes massive disruption of preformed *A. baumannii* biofilm. These findings pave the way to the repurposing of GaN as an antibiofilm agent for *A. baumannii*.

KEYWORDS *Acinetobacter baumannii*, biofilm, gallium, serum, iron, iron metabolism

Received 19 July 2016 **Returned for modification** 8 September 2016 **Accepted** 26 October 2016

Accepted manuscript posted online 31 October 2016

Citation Runci F, Bonchi C, Frangipani E, Visaggio D, Visca P. 2017. *Acinetobacter baumannii* biofilm formation in human serum and disruption by gallium. Antimicrob Agents Chemother 61:e01563-16. https://doi.org/10.1128/AAC.01563-16.

Address correspondence to Paolo Visca, paolo.visca@uniroma3.it.

Acinetobacter baumannii is an important cause of nosocomial infection, especially among critically ill patients in intensive care units (ICUs) (1). Three international clonal lineages (ICLs) are responsible for the majority of *A. baumannii* infections worldwide (2). Recent isolates belonging to these epidemic lineages invariably disclose a multidrug-resistant (MDR) phenotype, which narrows the therapeutic options (3, 4), resulting in higher mortality (5, 6).

In the search for new anti-infective agents against *A. baumannii*, we have recently reported that gallium nitrate [$Ga(NO_3)_3$; GaN] inhibits *A. baumannii* growth *in vitro* and *in vivo* by interfering with bacterial iron metabolism (7), paving the way for the repurposing of Ganite (an FDA-approved formulation of GaN) for the treatment of pan-resistant or otherwise untreatable *A. baumannii* infections (8).

Many bacterial pathogens, including *A. baumannii*, can grow either as dispersed (planktonic) cells or as matrix-enclosed communities called biofilms. The ability to form biofilm is shared among clinical *A. baumannii* isolates, likely because the biofilm mode of growth contributes to the ecological success of this pathogen in the hospital (1, 9, 10). Biofilm promotes adhesion and facilitates long-term survival of *A. baumannii* on both biotic and abiotic surfaces (11, 12). Cells encased in biofilms are characterized by low metabolic activity and are protected by the extracellularly secreted matrix, which makes them less susceptible to antibiotics and to components of the host innate immunity (13). *A. baumannii* frequently causes biofilm-related infections, especially ventilator-associated pneumonia and catheter-related infection, which can be extremely refractory to antibiotic treatment (1, 14).

We have recently shown that complement-free human serum (HS) supports the planktonic growth of *A. baumannii*, likely reflecting the propensity of this species for bacteremic spread (7). Since biofilm-related infections are primary sources for systemic dissemination, in this work we investigate the ability of *A. baumannii* to form mature biofilms also in HS. We also provide evidence that GaN treatment disrupts preformed *A. baumannii* biofilms.

RESULTS

***A. baumannii* growth and biofilm formation in HS.** The ability of *A. baumannii* to generate biofilm was initially assessed in Mueller-Hinton (MH) broth at 37°C for 48 h by

TABLE 1 Characteristics of *A. baumannii* strains used in this study

Strain	Country of origin	Year(s)	Source	ICL (ST)[a]	Resistance[b]	GaN IC_{90} (μM)[c]	Biofilm (OD_{600})[d]	Reference
ATCC 19606^T	USA	1948	Urine	Non-ICL (931)	Susceptible	ND	0.108 ± 0.007	36
ATCC 17978	France	1951	Blood	Non-ICL (959)	Susceptible	3.8 ± 0.0	0.044 ± 0.011	37
AYE	France	2001	Urine	1 (231)	MDR	10.7 ± 1.3	0.069 ± 0.011	38
A458	Estonia	2001–2004	Clinical (ARPAC project)	1 (NA)	MDR	21.2 ± 1.7	0.104 ± 0.012	39
A472	Poland	2001–2004	Clinical (ARPAC project)	1 (245)	MDR	7.5 ± 0.4	0.120 ± 0.016	39
C13-373	Italy	2007	Blood	1 (95)	MDR	31.0 ± 3.2	0.142 ± 0.018	40
C6-397	Italy	2007	Blood	1 (196)	MDR	28.9 ± 0.2	0.133 ± 0.019	40
ACICU	Italy	2005	Cerebrospinal fluid	2 (437)	MDR	14.0 ± 2.1	0.134 ± 0.012	16
A60	Argentina	2001–2004	Clinical (ARPAC project)	2 (241)	MDR	7.7 ± 0.1	0.148 ± 0.022	40
A491	India	2001–2004	Clinical (ARPAC project)	2 (NA)	MDR	14.0 ± 2.3	0.085 ± 0.020	40
LUH5875	The Netherlands	1997	Blood	3 (NA)[e]	MDR	14.5 ± 5.2	0.104 ± 0.020	41
A377	Germany	2001–2004	Clinical (ARPAC project)	3 (187)	MDR	4.0 ± 0.0	0.120 ± 0.015	40

[a]ICL, international clonal lineage; ST, sequence type according to the multilocus sequence typing (MLST) Oxford scheme (http://pubmlst.org/abaumannii/); NA, not assigned.
[b]MDR, multidrug resistant.
[c]The IC_{90} in HS was determined as described by Antunes et al. (7);.ND, not determined due to poor growth.
[d]Biofilm formation was determined after 48-h growth in MH broth.
[e]ST3 according to the MLST Pasteur scheme (http://pubmlst.org/abaumannii/).

the use of a 96-well microtiter plate assay (15). Ten *A. baumannii* multidrug-resistant (MDR) clinical isolates, representing the main ICLs, were selected for this purpose (Table 1). The *A. baumannii* type strains ATCC 19606^T and the reference strain ATCC 17978 were also included in the screening panel (Table 1). All *A. baumannii* isolates showed the ability to form biofilms in MH broth although to different extents (optical density at 600 nm [OD_{600}] range of 0.044 to 0.148) (Table 1). Then the ability of *A. baumannii* to grow and form biofilm in HS was investigated. All isolates, except the type strain ATCC 19606^T, were able to grow in HS (Fig. 1), and fewer than half of them (C13-373, ACICU, A60, A491, and A377) developed substantial biofilm levels (OD_{600} of $>$0.070) (Fig. 1). Since HS is sensed by *A. baumannii* as an iron-poor medium (7), we tested the effect of exogenously added iron on bacterial growth and biofilm formation. In nearly

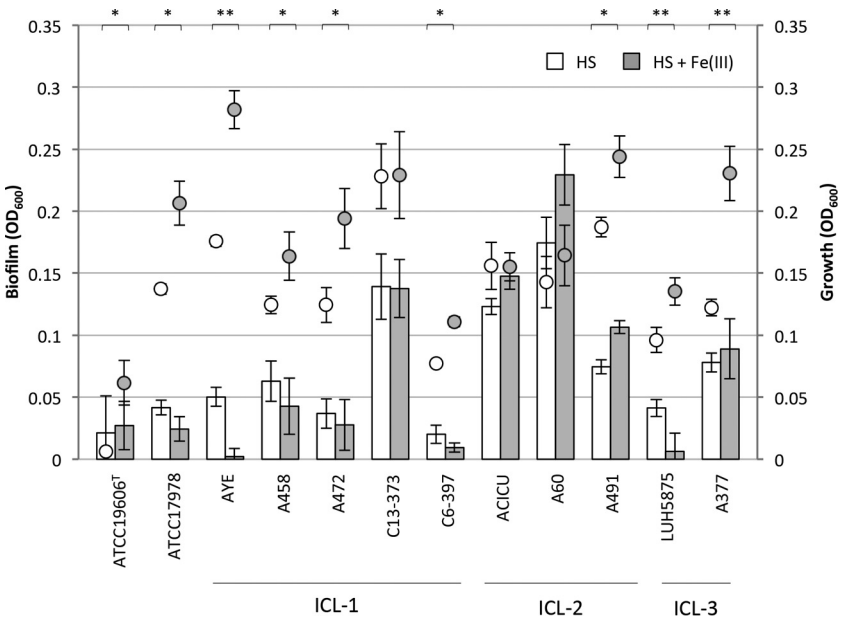

FIG 1 Growth and biofilm formation in HS by clinical *A. baumannii* isolates. *A. baumannii* growth (circles) and biofilm (bars) in HS and in HS supplemented with 100 μM $FeCl_3$ were determined. Growth was measured spectrophotometrically (OD_{600}), and biofilm formation was determined after a 72-h incubation at 37°C using a CV assay. Values represent the means (± standard deviations) of three independent assays. Asterisks denote statistically significant growth differences (*, $P < 0.05$; **, $P < 0.005$; Student's *t* test).

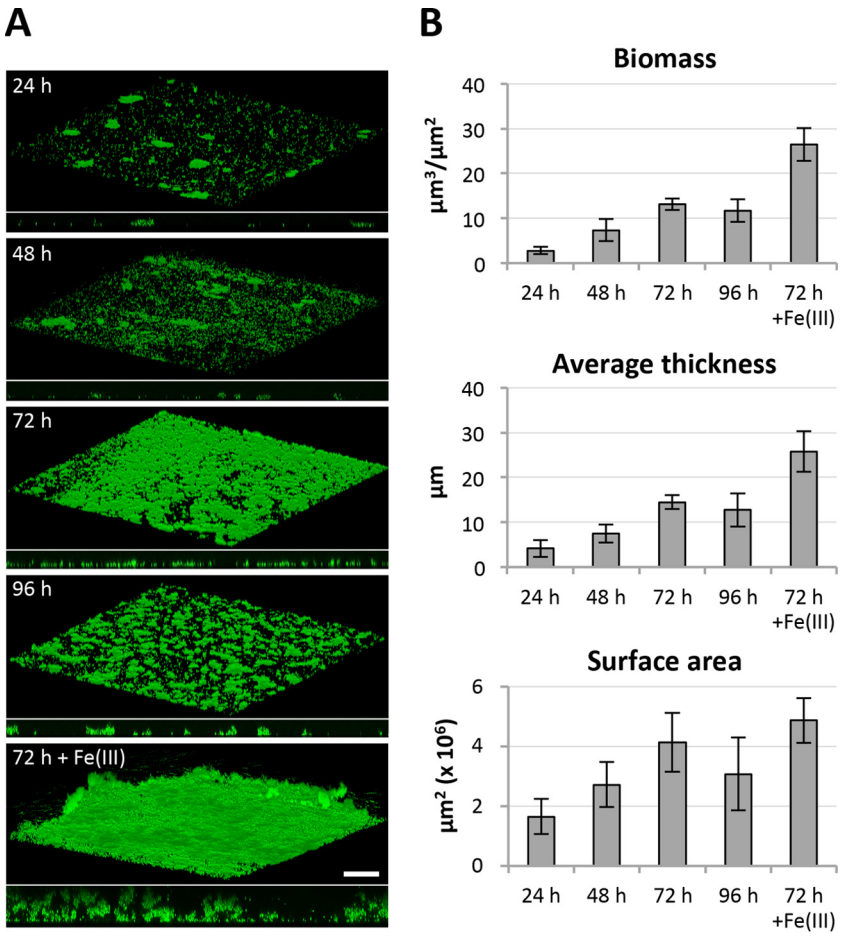

FIG 2 Time course of *A. baumannii* ACICU biofilm formation in HS. (A) Representative confocal microscope images of biofilms (*x-y* plane and side view) stained with acridine orange. (B) Quantification of biofilm spatial characteristics determined by analysis with COMSTAT, version 2.1. Five image stacks were analyzed per condition. Scale bar, 50 μm. +Fe(III), HS supplemented with 100 μM $FeCl_3$.

all isolates, the addition of 100 μM $FeCl_3$ to HS significantly stimulated bacterial growth. However, iron availability influenced *A. baumannii* biofilm formation in a strain-dependent manner, stimulating or reducing biofilm formation or having no effect (Fig. 1). Indeed, a good correlation ($r_s = 0.72$, $P < 0.05$) between growth yields and biofilm levels was observed for HS (see Fig. S1A in the supplemental material) but not for iron-supplemented HS (Fig. S1B).

To gain more insight into the dynamics of *A. baumannii* biofilm formation in HS, the invasive MDR clinical isolate ACICU (ICL-2, sequence type 437 [ST437]) (16) was initially chosen as a model organism since it produces elevated biofilm levels. Tridimensional biofilm development in HS was investigated by confocal microscopy using eight-well glass chamber slides incubated at 37°C for up to 96 h (17). Under these conditions, patches of *A. baumannii* cell aggregates became visible at 24 h postinoculum in HS, progressively expanding to attain a thick and confluent layer after 72 h and then starting dispersion at 96 h (Fig. 2A). Biofilm architecture analysis indicated that biomass progressively developed for up to 72 h, reaching a maximum of 13 $\mu m^3/\mu m^2$, concomitant with an increase of thickness and surface area (14 μm and 4.0×10^6 μm^2, respectively) (Fig. 2B). The decrease of all biofilm spatial characteristics observed after 96 h is likely due to nutrient exhaustion and consequent dispersal of the mature biofilm, consistent with the overall dynamics revealed by confocal microscopy observations (Fig. 2A). ACICU biofilm formation was stimulated by the addition of 100 μM $FeCl_3$ to HS, with an increase in all spatial characteristics at 72 h (Fig. 2A and B).

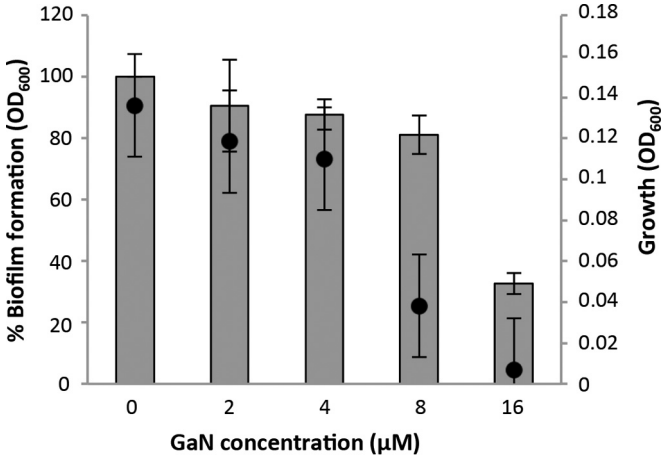

FIG 3 Effect of GaN on *A. baumannii* biofilm formation in HS. *A. baumannii* ACICU growth (circles) and biofilm formation (bars) in the presence of increasing concentrations of GaN (0 to 16 μM) were determined. Growth was measured spectrophotometrically (OD_{600}), and biofilm formation was determined using a CV assay after a 48-h incubation at 37°C. Values represent the means (± standard deviations) of three independent assays.

GaN inhibits planktonic growth of *A. baumannii* ACICU without preventing biofilm formation in HS. A microtiter plate assay (15) was used to investigate the inhibitory effect of GaN on *A. baumannii* ACICU planktonic growth and biofilm formation. We observed that 16 μM GaN strongly inhibited both planktonic and biofilm growth of *A. baumannii* ACICU in HS (Fig. 3). Notably, planktonic growth was inhibited by 72% in the presence of 8 μM GaN, whereas only a 20% biofilm reduction was observed at this GaN concentration.

GaN disrupts preformed *A. baumannii* biofilms in HS. For a preliminary assessment of the biofilm-disrupting activity of GaN, *A. baumannii* ACICU mature biofilms were developed for 72 h in HS in eight-well chamber slides and then challenged with increasing GaN concentrations (16, 32, and 64 μM in HS) for 48 and 72 h prior to analysis by confocal microscopy (Fig. 4A). GaN caused evident disruption of preformed

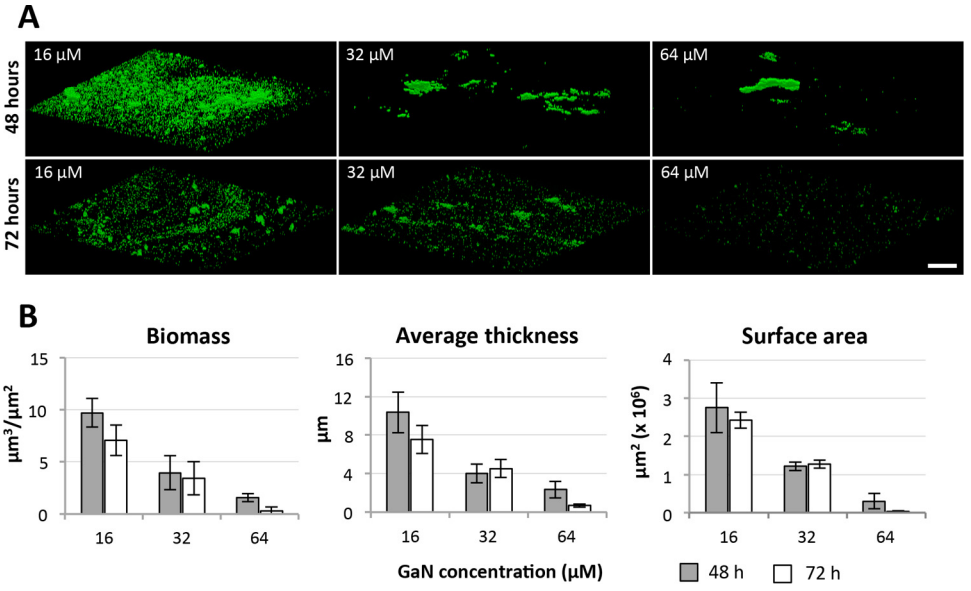

FIG 4 Effect of GaN on *A. baumannii* biofilm disruption in HS. (A) Representative confocal microscope images of *A. baumannii* biofilm developed for 72 h in HS at 37°C and then treated with the indicated GaN concentration (16 to 64 μM) for 48 h and 72 h at 37°C. (B) Quantification of biofilm spatial characteristics determined by analysis with COMSTAT, version 2.1. Five image stacks were analyzed per condition. Scale bar, 50 μm.

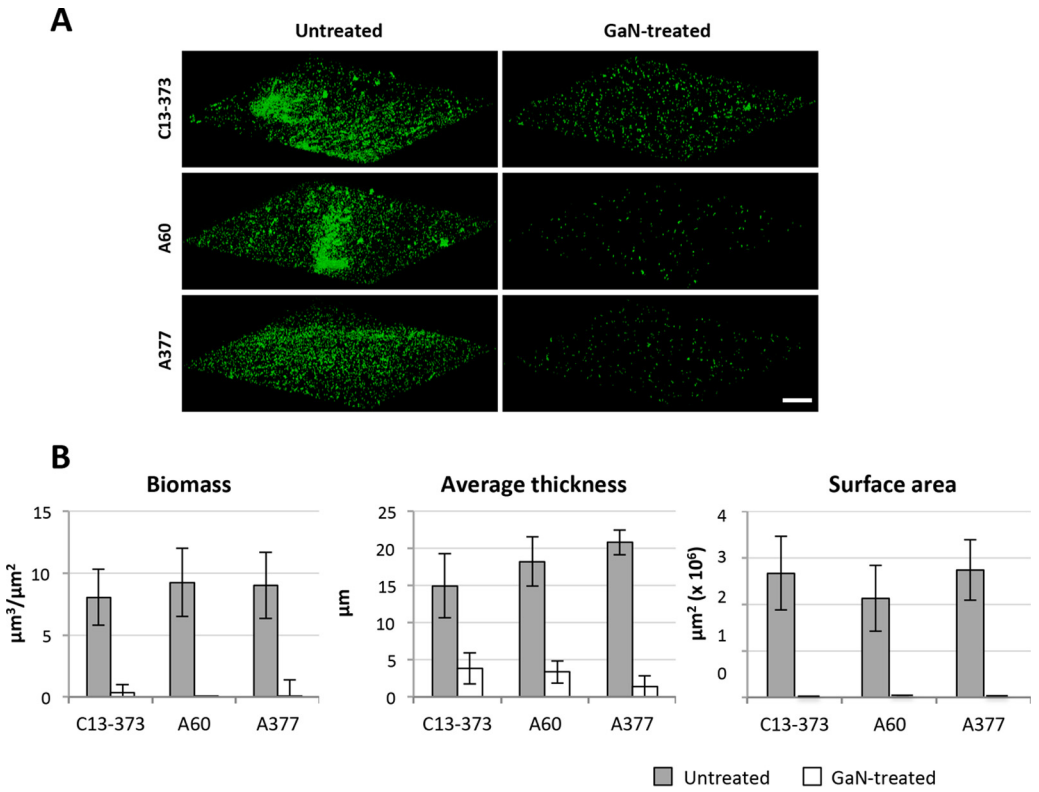

FIG 5 GaN disrupts the biofilm formed in HS by clinical *A. baumannii* isolates. (A) Representative confocal microscope images of *A. baumannii* A60, A377, and C13-373 biofilms developed for 72 h in HS at 37°C (left panels) and then treated with 64 μM GaN for 72 h at 37°C (right panels). (B) Quantification of biofilm spatial characteristics determined by analysis with COMSTAT, version 2.1. Five image stacks were analyzed per condition. Scale bar, 50 μm.

ACICU biofilms in a concentration-dependent manner (Fig. 4A), consistent with a reduction in biofilm biomass, average thickness, and surface area (Fig. 4B). Notably, treatment with 64 μM GaN resulted in nearly complete removal of glass-attached structures after 72 h (Fig. 4A), whereas GaN had no biofilm-disrupting effect in HS supplemented with 100 μM $FeCl_3$ (Fig. S2).

The biofilm-disrupting activity of GaN was further investigated using a selection of MDR clinical isolates belonging to ICL-1 (C13-373), ICL-2 (A60), and ICL-3 (A377). These isolates formed substantial biofilm levels in HS (OD_{600} of $>$0.070) (Fig. 1) and were characterized by different 90% inhibitory concentrations (IC_{90}s) of GaN (4.0 to 31.0 μM) (Table 1). Based on the results obtained with strain ACICU, bacteria were grown in HS for 72 h in eight-well chamber slides to allow the development of mature biofilms, as confirmed by confocal microscopy analysis (Fig. 5A). Then preformed biofilms were challenged with 64 μM GaN in HS for 72 h. Similar to what was observed with the prototypic strain ACICU, 64 μM GaN caused massive biofilm disruption, resulting in a strong reduction in biofilm mass, thickness, and surface area for all three MDR isolates tested (Fig. 5B). It should be noted that biofilm formed by isolate C13-373 in HS was almost completely disrupted by a GaN concentration approximately twice the IC_{90}.

DISCUSSION

To our knowledge, this study provides the first demonstration that epidemic MDR *A. baumannii* isolates can adopt a biofilm mode of growth when exposed to HS. This finding has relevant clinical implications, given that indwelling medical devices are primary colonization sites for *A. baumannii* and represent a major source for systemic dissemination (18).

Previous experiments have demonstrated that HS is sensed by *A. baumannii* as an iron-poor environment (7). Thus, the ability of epidemic MDR *A. baumannii* isolates to

multiply in HS implies that this organism can overcome the nutritional stress imposed by the host's iron-withholding defenses (19). Another important observation is that some epidemic MDR *A. baumannii* isolates can form a biofilm during growth in HS. For most isolates, biofilm levels in HS were lower than in those MH broth (Table 1 and Fig. 1), whereas isolates C13-373 (ICL-1), ACICU, and A60 (ICL-2) generated comparably high biofilm levels under both conditions. In this context, it must be pointed out that biofilm testing in HS should provide a more realistic view of the biofilm-generating potential of individual strains *in vivo* than observations made using laboratory media. While iron supplementation had an overall stimulating effect on *A. baumannii* growth in HS, it was not perceived as a biofilm-inducing signal by nearly half of the strains tested. This is consistent with the previously reported variability in the response of *A. baumannii* biofilms to iron (9).

Bacterial biofilms are known for being extremely refractory to antibiotic treatments, thereby posing a serious challenge to the clinical management of biofilm-associated infections (13, 20). Thus, an important added value of any antimicrobial drug resides in its ability to prevent biofilm formation and/or eradicate a preformed biofilm. Given the importance of iron in host-pathogen interactions, drugs interfering with microbial iron metabolism represent viable candidates for the development of new antibacterials (21). In this work, we provide evidence that gallium, which behaves as an iron-mimetic metal (22), is endowed with potent antibiofilm properties in addition to its previously reported ability to inhibit *A. baumannii* planktonic growth (7, 23). The antimicrobial activity of GaN is dependent on the growth medium as this activity is invariably abrogated in an iron-rich medium, such as MH broth (7, 8, 22). This reinforces the rationale of testing the antibiofilm properties of GaN in HS. While GaN was effective in inhibiting *A. baumannii* planktonic growth in HS at concentrations ranging from 3.8 to 31 μM (IC_{90} values are given in Table 1), it had no biofilm-preventing activity on the prototypic strain ACICU upon challenge with subinhibitory GaN concentrations (Fig. 3). Intriguingly, a moderate shift toward the biofilm mode of growth was observed under this condition, plausibly as the result of GaN-induced cellular stress. However, a remarkable (ca. 3.5-fold) reduction of preformed ACICU biofilm was observed after a 72-h exposure to 32 μM GaN, i.e., close to the peak concentration of gallium achievable in serum of patients undergoing Ganite treatment for cancer-related hypercalcemia (24). From an *in vivo* perspective, it is also tempting to speculate that the complement-dependent bactericidal activity of naive serum could synergize with gallium, thus potentiating its antibacterial and antibiofilm effects.

The biofilm-disrupting properties of GaN were strengthened by investigations on representative *A. baumannii* isolates selected from among those producing high biofilm levels in HS (Fig. 1). Following GaN exposure, a strong decrease in all biofilm spatial characteristics was observed for all isolates tested (C13-373, ACICU, A60, and A377), irrespective of their belonging to different ICLs (Fig. 4 and 5) and having different GaN IC_{90}s (Table 1).

The inherent ability of *A. baumannii* epidemic strains to form biofilm in HS represents a serious concern for clinicians, given that the use of invasive procedures in ICUs (e.g., intravascular and urinary catheters and drainage and mechanical ventilation tubes) has been listed as a major risk factor for *A. baumannii* infection (25, 26). The antimicrobial properties of metals have been exploited to generate metal-doped matrixes for the coating of medical devices, and controlled release of antibacterial metals from implantable materials has been shown to reduce bacterial colonization (27, 28). We believe that the potent antibacterial and antibiofilm properties of gallium, combined with its good biocompatibility, make this iron-mimetic metal a suitable candidate for the coating of biomaterials and indwelling medical devices. In support of this possibility, a number of recent reports have highlighted the efficacy of gallium-doped materials in counteracting surface proliferation of some pathogenic bacteria, including *A. baumannii* (29–32).

Finally, while gallium activity can be potentiated by complexation with suitable

carriers (23), a potential advantage of GaN is that Ganite (the FDA-approved formulation) could readily be repositioned for off-label treatment of *A. baumannii* infection.

MATERIALS AND METHODS

Bacterial strains and growth media. *A. baumannii* strains used in this study are listed in Table 1. Bacteria were grown in Mueller-Hinton (MH) broth, Chelex 100-treated Trypticase soy broth dialysate (TSBD) medium (33), or complement-free human serum (HS). Human serum was obtained from 125 healthy donors, following illustration, approval, and subscription of an informed consent. The serum sampling protocol was approved by the review board of Policlinico Umberto I, Sapienza University, Rome. Serum samples were pooled, complement was inactivated by incubation at 56°C for 30 min, and the bulk of HS was sterilized by filtration, as previously described (7), and then stored at +4°C until used. Bulk HS chemistry was as follows: total serum proteins, 80 mg/ml; total iron, 0.70 μg/ml; ferritin, 0.243 μg/ml; transferrin (Tf), 2.63 mg/ml; total iron binding capacity, 4.27 mg/ml (20% Tf saturation). Iron chloride ($FeCl_3$) and GaN were added when indicated in Fig. 1 and 2 ($FeCl_3$), Fig. 3 to 5 (GaN), and Fig. S2 ($FeCl_3$ and GaN).

Growth, biofilm formation, and GaN susceptibility tests. Bacterial cultures grown for ≈16 h in MH broth or TSBD were diluted to an OD_{600} of 0.01 in 100 μl of MH or HS, respectively, and grown for 48 and/or 72 h at 37°C in 96-well microtiter plates, with gentle shaking (110 rpm). Growth was monitored spectrophotometrically (OD_{600}), and biofilm formation was quantified by a microtiter plate assay (15). Briefly, planktonic cells were removed, and the attached cells were gently washed with sterile saline solution, air dried, and stained for 30 min with 150 μl of 0.1% crystal violet (CV) in water. Wells were then gently washed twice with water, and the surface-associated dye was dissolved in 200 μl of 96% ethanol for 20 min at 4°C to prevent ethanol evaporation. The OD_{600} of the CV eluate was measured in a Wallac 1420 Victor 3V multilabel plate reader (PerkinElmer).

To determine the effect of GaN on *A. baumannii* planktonic growth and biofilm formation, strain ACICU was grown in 96-well microtiter plates containing 100 μl of HS supplemented with increasing GaN concentrations (0 to 16 μM) and incubated for 48 h and 72 h at 37°C.

The GaN concentration that inhibited growth by 90% (IC_{90}) in HS was determined as previously described (7). When indicated in Fig. 1 and 2 and Fig. S2, cultures were supplemented with 100 μM $FeCl_3$.

Confocal microscopy analyses of biofilm formation and disruption. Bacteria were inoculated at an OD_{600} of 0.01 in 200 μl of HS in an eight-well chamber slide (Thermo Fisher Scientific) (17) and incubated at 37°C under static conditions. To visualize biofilm structures, after biofilm was stained with acridine orange, each well was filled with saline solution, and the coverslip was sealed to the slide. Biofilms were observed with a Leica TCS SP5 confocal microscope, and biofilm spatial characteristics were quantified using COMSTAT, version 2.1 (34, 35), by analyzing at least five image stacks per condition.

For quantification of biofilm disruption in HS, bacteria were inoculated at an OD_{600} of 0.01 in 200 μl of HS, incubated at 37°C for 72 h to allow biofilm formation, and then challenged with HS supplemented with GaN (16 μM, 32 μM and 64 μM) and 100 μM $FeCl_3$, as indicated in Fig. 4 and 5 and Fig. S2. Microscopy analyses were performed after 48 h and 72 h of treatment, depending on the *A. baumannii* strains tested, as described above.

Statistical analysis. A Student *t* test was used to determine the significance of differences in *A. baumannii* growth levels. Spearman's coefficient (r_s) was used to determine the correlation between growth and biofilm levels. Statistical analyses were performed using GraphPad Prism software.

SUPPLEMENTAL MATERIAL

Supplemental material for this article may be found at https://doi.org/10.1128/AAC.01563-16.

TEXT S1, PDF file, 1.1 MB.

ACKNOWLEDGMENTS

This work was supported by a PRIN grant (protocol 2012WJSX8K) from the Ministero dell'Istruzione dell'Università e della Ricerca (MIUR) to P.V.

We thank the personnel from Policlinico Umberto I, Sapienza University of Rome, for help in collecting blood samples from healthy donors.

REFERENCES

1. Dijkshoorn L, Nemec A, Seifert H. 2007. An increasing threat in hospitals: multidrug-resistant *Acinetobacter baumannii*. Nat Rev Microbiol 5:1–8. https://doi.org/10.1038/nrmicro1789.
2. Antunes LC, Visca P, Towner KJ. 2014. *Acinetobacter baumannii*: evolution of a global pathogen. Pathog Dis 71:292–301. https://doi.org/10.1111/2049-632X.12125.
3. Diancourt L, Passet V, Nemec A, Dijkshoorn L, Brisse S. 2010. The population structure of *Acinetobacter baumannii*: expanding multiresistant clones from an ancestral susceptible genetic pool. PLoS One 5:e10034. https://doi.org/10.1371/journal.pone.0010034.
4. Zarrilli R, Pournaras S, Giannouli M, Tsakris A. 2013. Global evolution of multidrug-resistant *Acinetobacter baumannii* clonal lineages. Int J Antimicrob Agents 41:11–19. https://doi.org/10.1016/j.ijantimicag.2012.09.008.
5. Falagas ME, Kopterides P, Siempos II. 2006. Attributable mortality of *Acinetobacter baumannii* infection among critically ill patients. Clin Infect Dis 43:389–390. https://doi.org/10.1086/505599.
6. Seifert H, Strate A, Pulverer G. 1995. Nosocomial bacteremia due to *Acinetobacter baumannii*. Clinical features, epidemiology, and predictors of mortality. Medicine (Baltimore) 74:340–349.

7. Antunes LC, Imperi F, Minandri F, Visca P. 2012. *In vitro* and *in vivo* antimicrobial activities of gallium nitrate against multidrug-resistant *Acinetobacter baumannii*. Antimicrob Agents Chemother 56:5961–5970. https://doi.org/10.1128/AAC.01519-12.
8. Bonchi C, Imperi F, Minandri F, Visca P, Frangipani E. 2014. Repurposing of gallium-based drugs for antibacterial therapy. Biofactors 40:303–312. https://doi.org/10.1002/biof.1159.
9. Gentile V, Frangipani E, Bonchi C, Minandri F, Runci F, Visca P. 2014. Iron and *Acinetobacter baumannii* biofilm formation. Pathogens 3:704–719. https://doi.org/10.3390/pathogens3030704.
10. Lee HW, Koh YM, Kim J, Lee JC, Lee YC, Seol SY, Cho DT, Kim J. 2008. Capacity of multidrug-resistant clinical isolates of *Acinetobacter baumannii* to form biofilm and adhere to epithelial cell surfaces. Clin Microbiol Infect 14:49–54. https://doi.org/10.1111/j.1469-0691.2007.01842.x.
11. Gaddy JA, Actis LA. 2009. Regulation of *Acinetobacter baumannii* biofilm formation. Future Microbiol 4:273–278. https://doi.org/10.2217/fmb.09.5.
12. Tomaras AP, Dorsey CW, Edelmann RE, Actis LA. 2003. Attachment to and biofilm formation on abiotic surfaces by *Acinetobacter baumannii*: involvement of a novel chaperone-usher pili assembly system. Microbiology 149:3473–3484. https://doi.org/10.1099/mic.0.26541-0.
13. Davies D. 2003. Understanding biofilm resistance to antibacterial agents. Nat Rev Drug Discov 2:114–122. https://doi.org/10.1038/nrd1008.
14. Pour NK, Dusane DH, Dhakephalkar PK, Zamin FR, Zinjarde SS, Chopade BA. 2011. Biofilm formation by *Acinetobacter baumannii* strains isolated from urinary tract infection and urinary catheters. FEMS Immunol Med Microbiol 62:328–338. https://doi.org/10.1111/j.1574-695X.2011.00818.x.
15. O'Toole G, Kaplan HB, Kolter R. 2000. Biofilm formation as microbial development. Annu Rev Microbiol 54:49–79. https://doi.org/10.1146/annurev.micro.54.1.49.
16. Iacono M, Villa L, Fortini D, Bordoni R, Imperi F, Bonnal RJ, Sicheritz-Ponten T, De Bellis G, Visca P, Cassone A, Carattoli A. 2008. Whole-genome pyrosequencing of an epidemic multidrug-resistant *Acinetobacter baumannii* strain belonging to the European clone II group. Antimicrob Agents Chemother 52:2616–2625. https://doi.org/10.1128/AAC.01643-07.
17. Jurcisek JA, Dickson AC, Bruggeman ME, Bakaletz LO. 2011. *In vitro* biofilm formation in an 8-well chamber slide. J Vis Exp 47:e2481.
18. Cisneros JM, Rodríguez-Baño J. 2002. Nosocomial bacteremia due to *Acinetobacter baumannii*: epidemiology, clinical features and treatment. Clin Microbiol Infect 8:687–693. https://doi.org/10.1046/j.1469-0691.2002.00487.x.
19. Weinberg ED. 2009. Iron availability and infection. Biochim Biophys Acta 1790:600–605. https://doi.org/10.1016/j.bbagen.2008.07.002.
20. Hall-Stoodley L, Costerton JW, Stoodley P. 2004. Bacterial biofilms: from the natural environment to infectious diseases. Nat Rev Microbiol 2:95–108. https://doi.org/10.1038/nrmicro821.
21. Foley TL, Simeonov A. 2012. Targeting iron assimilation to develop new antibacterials. Expert Opin Drug Discov 7:831–847. https://doi.org/10.1517/17460441.2012.708335.
22. Minandri F, Bonchi C, Frangipani E, Imperi F, Visca P. 2014. Promises and failures of gallium as an antibacterial agent. Future Microbiol 9:379–397. https://doi.org/10.2217/fmb.14.3.
23. Arivett BA, Fiester SE, Ohneck EJ, Penwell WF, Kaufman CM, Relich RF, Actis LA. 2015. Antimicrobial activity of gallium protoporphyrin IX against *Acinetobacter baumannii* strains displaying different antibiotic resistance phenotypes. Antimicrob Agents Chemother 59:7657–7665. https://doi.org/10.1128/AAC.01472-15.
24. Chitambar CR. 2010. Medical applications and toxicities of gallium compounds. Int J Environ Res Public Health 7:2337–2361. https://doi.org/10.3390/ijerph7052337.
25. Falagas ME, Kopterides P. 2006. Risk factors for the isolation of multidrug-resistant *Acinetobacter baumannii* and *Pseudomonas aeruginosa*: a systematic review of the literature. J Hosp Infect 64:7–15. https://doi.org/10.1016/j.jhin.2006.04.015.
26. García-Garmendia JL, Ortiz-Leyba C, Garnacho-Montero J, Jiménez-Jiménez FJ, Pérez-Paredes C, Barrero-Almodóvar AE, Gili-Miner M. 2001. Risk factors for *Acinetobacter baumannii* nosocomial bacteremia in critically ill patients: a cohort study. Clin Infect Dis 33:939–946. https://doi.org/10.1086/322584.
27. Bayramov DF, Neff JA. 3 August 2016. Beyond conventional antibiotics: new directions for combination products to combat biofilm. Adv Drug Deliv Rev https://doi.org/10.1016/j.addr.2016.07.010.
28. Hetrick EM, Schoenfisch MH. 2006. Reducing implant-related infections: active release strategies. Chem Soc Rev 35:780–789. https://doi.org/10.1039/b515219b.
29. Cochis A, Azzimonti B, Della Valle C, De Giglio E, Bloise N, Visai L, Cometa S, Rimondini L, Chiesa R. 2016. The effect of silver or gallium doped titanium against the multidrug resistant *Acinetobacter baumannii*. Biomaterials 80:80–95. https://doi.org/10.1016/j.biomaterials.2015.11.042.
30. Herron M, Schurr MJ, Murphy CJ, McAnulty JF, Czuprynski CJ, Abbott NL. 2015. Gallium-loaded dissolvable microfilm constructs that provide sustained release of Ga^{3+} for management of biofilms. Adv Healthc Mater 4:2849–2859. https://doi.org/10.1002/adhm.201500599.
31. Ma H, Darmawan ET, Zhang M, Zhang L, Bryers JD. 2013. Development of a poly(ether urethane) system for the controlled release of two novel anti-biofilm agents based on gallium or zinc and its efficacy to prevent bacterial biofilm formation. J Control Release 172:1035–1044. https://doi.org/10.1016/j.jconrel.2013.10.005.
32. Valappil SP, Yiu HH, Bouffier L, Hope CK, Evans G, Claridge JB, Higham SM, Rosseinsky MJ. 2013. Effect of novel antibacterial gallium-carboxymethyl cellulose on *Pseudomonas aeruginosa*. Dalton Trans 42:1778–1786. https://doi.org/10.1039/C2DT32235H.
33. Ohman DE, Sadoff JC, Iglewski BH. 1980. Toxin A-deficient mutants of *Pseudomonas aeruginosa* PA103: isolation and characterization. Infect Immun 28:899–908.
34. Heydorn A, Nielsen AT, Hentzer M, Sternberg C, Givskov M, Ersbøll BK, Molin S. 2000. Quantification of biofilm structures by the novel computer program COMSTAT. Microbiology 146:2395–2407. https://doi.org/10.1099/00221287-146-10-2395.
35. Vorregaard M. 2008. Comstat2—a modern 3D image analysis environment for biofilms, in informatics and mathematical modelling. Technical University of Denmark, Kongens Lyngby, Denmark.
36. Janssen P, Maquelin K, Coopman R, Tjernberg I, Bouvet P, Kersters K, Dijkshoorn L. 1997. Discrimination of *Acinetobacter* genomic species by AFLP fingerprinting. Int J Syst Bacteriol 47:1179–1187. https://doi.org/10.1099/00207713-47-4-1179.
37. Smith MG, Gianoulis TA, Pukatzki S, Mekalanos JJ, Ornston LN, Gerstein M, Snyder M. 2007. New insights into *Acinetobacter baumannii* pathogenesis revealed by high-density pyrosequencing and transposon mutagenesis. Genes Dev 21:601–614. https://doi.org/10.1101/gad.1510307.
38. Poirel L, Menuteau O, Agoli N, Cattoen C, Nordmann P. 2003. Outbreak of extended-spectrum beta-lactamase VEB-1-producing isolates of *Acinetobacter baumannii* in a French hospital. J Clin Microbiol 41:3542–3547. https://doi.org/10.1128/JCM.41.8.3542-3547.2003.
39. Towner KJ, Levi K, Vlassiadi M, ARPAC Steering Group. 2008. Genetic diversity of carbapenem-resistant isolates of *Acinetobacter baumannii* in Europe. Clin Microbiol Infect 14:161–167. https://doi.org/10.1111/j.1469-0691.2007.01911.x.
40. Migliavacca R, Espinal P, Principe L, Drago M, Fugazza G, Roca I, Nucleo E, Bracco S, Vila J, Pagani L, Luzzaro F. 2013. Characterization of resistance mechanisms and genetic relatedness of carbapenem-resistant *Acinetobacter baumannii* isolated from blood, Italy. Diagn Microbiol Infect Dis 75:180–186. https://doi.org/10.1016/j.diagmicrobio.2012.11.002.
41. van Dessel H, Dijkshoorn L, van der Reijden T, Bakker N, Paauw A, van den Broek P, Verhoef J, Brisse S. 2004. Identification of a new geographically widespread multiresistant *Acinetobacter baumannii* clone from European hospitals. Res Microbiol 155:105–112. https://doi.org/10.1016/j.resmic.2003.10.003.